International Journal of Multiphase Flow 36 (2010) 588–597

Contents lists available at ScienceDirect

International Journal of Multiphase Flow

journal homepage: www.elsevier.com/locate/ijmulflow

Experimental investigation of two-phase discharge from a stratified region through a small branch mounted on an inclined wall

J.T. Bartley, H.M. Soliman *, G.E. Sims

Department of Mechanical and Manufacturing Engineering, University of Manitoba, Winnipeg, Manitoba, Canada R3T 5V6

ARTICLE INFO

Article history:
Received 21 November 2009
Received in revised form 6 March 2010
Accepted 9 March 2010
Available online 15 March 2010

Keywords:
Two-phase discharge
Small branch
Inclined wall
Experimental data
Empirical correlation

ABSTRACT

Experimental data are presented for the mass flow rate and quality of two-phase discharge through a small branch of diameter d (=6.35 mm) attached normally to an inclined flat plane. The flat plane was situated in a large tank containing a stratified mixture of air and water under pressure (316 kPa) and at room temperature. The plane was inclined through various angles (θ) in increments of 30°, from the outlet-branch orientation being vertically upward through the horizontal to vertically downward. The bulk of the data correspond to seven inclination angles and two test-section-to-separator pressure differences (ΔP) of 11.0 and 115.5 kPa, and for each combination of θ and ΔP, the mass flow rate and quality were measured at different values of the interface level (h) between the onsets of gas and liquid entrainment. Four additional data sets were generated for other values of ΔP in order to confirm certain trends. Influences of these independent variables on the mass flow rate and quality are discussed and normalized plots are presented showing that the data can be collapsed for a wide range of conditions. Comparisons are made between the present data and previous correlations/models and new empirical correlations are formulated and shown to be capable of predicting the present data with good accuracy.

© 2010 Elsevier Ltd. All rights reserved.

1. Introduction

The flow distribution system in many industrial applications quite often involves two-phase flow discharging from a stratified region through branches mounted on flat walls or large circular pipes. Examples of these applications include the flow through small breaks in the horizontal cooling channels of nuclear reactors during postulated loss-of-coolant accidents (LOCA), the flow distribution in the CANDU (Canadian Deuterium and Uranium reactors) header–feeder system during accident scenarios, and two-phase distribution systems in general, where an incoming two-phase stream fed into a large header or chamber is divided among a number of discharging streams, as for instance, in a shell-and-tube heat exchanger. Knowledge of the flow phenomena involved and the ability to make accurate predictions of the mass flow rate and quality in the branch are obviously important for the proper and safe design of these systems.

The mass flow rate and quality of two-phase discharge from a stratified region depend on the location of the interface relative to the branch (Zuber, 1980). For high interface levels above the branch, the discharge flow will be in the form of single-phase liquid and, as the interface is lowered, a critical condition (onset of gas entrainment) is reached whereby gas begins being entrained in the liquid flow. The discharge continues to be in the form of two-phase flow as the interface height is decreased until a second critical condition (onset of liquid entrainment) is reached where liquid flow ceases and the discharge begins to be in the form of single-phase gas flow.

Determining the critical conditions at the onsets of gas and liquid entrainment, as well as the mass flow rate and quality in the two-phase region for various operating conditions are therefore essential for the design and analysis of pertinent systems. The need for such information has motivated significant research in the literature (e.g., Smoglie and Reimann, 1986; Schrock et al., 1986; Smoglie et al., 1987; Gardner, 1988; Yonomoto and Tasaka, 1988, 1991; Micaelli and Memponteil, 1989; Maciaszek and Micaelli, 1990; Hassan et al., 1998; Welter et al., 2004). These investigations produced experimental data, empirical correlations and theoretical models for the two onsets and the mass flow and quality of the two-phase discharge for the case of a single branch. Only the horizontal, vertically upward, and vertically downward branch orientations were considered in these studies. The case of multiple discharges was also considered because of its relevance to flow-distribution headers (e.g., Parrott et al., 1991; Armstrong et al., 1992; Hassan et al., 1996a,b, 1997; Teclemariam et al., 2003).

On the other hand, limited information currently exists for the case of branches with various inclination angles from the horizontal. Lee et al. (2007) reported experimental data on the onsets of gas and liquid entrainment in a single inclined branch attached

* Corresponding author. Tel.: +1 204 474 9307; +1 204 275 7507.
E-mail address: hsolima@cc.umanitoba.ca (H.M. Soliman).

0301-9322/$ - see front matter © 2010 Elsevier Ltd. All rights reserved.
doi:10.1016/j.ijmultiphaseflow.2010.03.002

to a horizontal header. Later, Bartley et al. (2008) reported experimental and empirical correlations for the onsets of gas and liquid entrainment in a single branch attached to a flat inclined wall covering a number of branch inclinations (from vertically upward to vertically downward) for both phenomena. The objective of the present investigation is to add to the work of Bartley et al. by generating experimental data and correlations for the two-phase mass flow rate and quality in a branch with various inclination angles. To the best of the authors' knowledge, no data of this type currently exist in the literature and, keeping in mind that small breaks may occur at any location around the circumference of a pipe or a flat retaining wall of a header, the need for such data is evident.

2. Experimental investigation

2.1. Experimental parameters

A set of schematic diagrams that defines the experimental parameters for the present system is shown in Fig. 1. A discharge branch of circular cross-section (diameter d) is mounted on an inclined wall bounding a region containing a stratified gas–liquid mixture at stagnation pressure P_o and stagnation temperature T_o. The wall is inclined at an angle θ from the vertical direction, as indicated in the figure. The positive sense of the angle θ is when the wall is inclined away from the interface, as viewed from the gas side, and the negative sense of the angle θ is when the wall is inclined towards the interface as viewed from the gas side. The intersection point between the plane of the wall and the centreline of the branch is the reference point from which the vertical distance h to the gas–liquid interface is measured. The vertical distance h is taken to be positive when the interface lies above the reference point and negative when the interface lies below the reference point. The discharging flow of gas and liquid is carried through a connecting line (not shown) to a separator where the pressure is maintained at P_s. The mass flow rate through the branch is controlled by the pressure difference ΔP, where $\Delta P = P_o - P_s$.

For a given condition of fixed P_o, T_o and ΔP, it is useful to consider the sequence of events that occurs with the discharge flow as the height of the interface h is changed. At high positive values of h, the discharge flow would be single-phase liquid, and the flow rate, $\dot{m}_L$, would be essentially independent of h. On decreasing h, a critical value is reached where gas begins being entrained in the flow of liquid; this is referred to as the onset of gas entrainment (OGE). At this condition, $h = h_{OGE}$ and $\dot{m}_L = \dot{m}_{L,OGE}$. Further lowering of the interface results in a steady two-phase discharge of

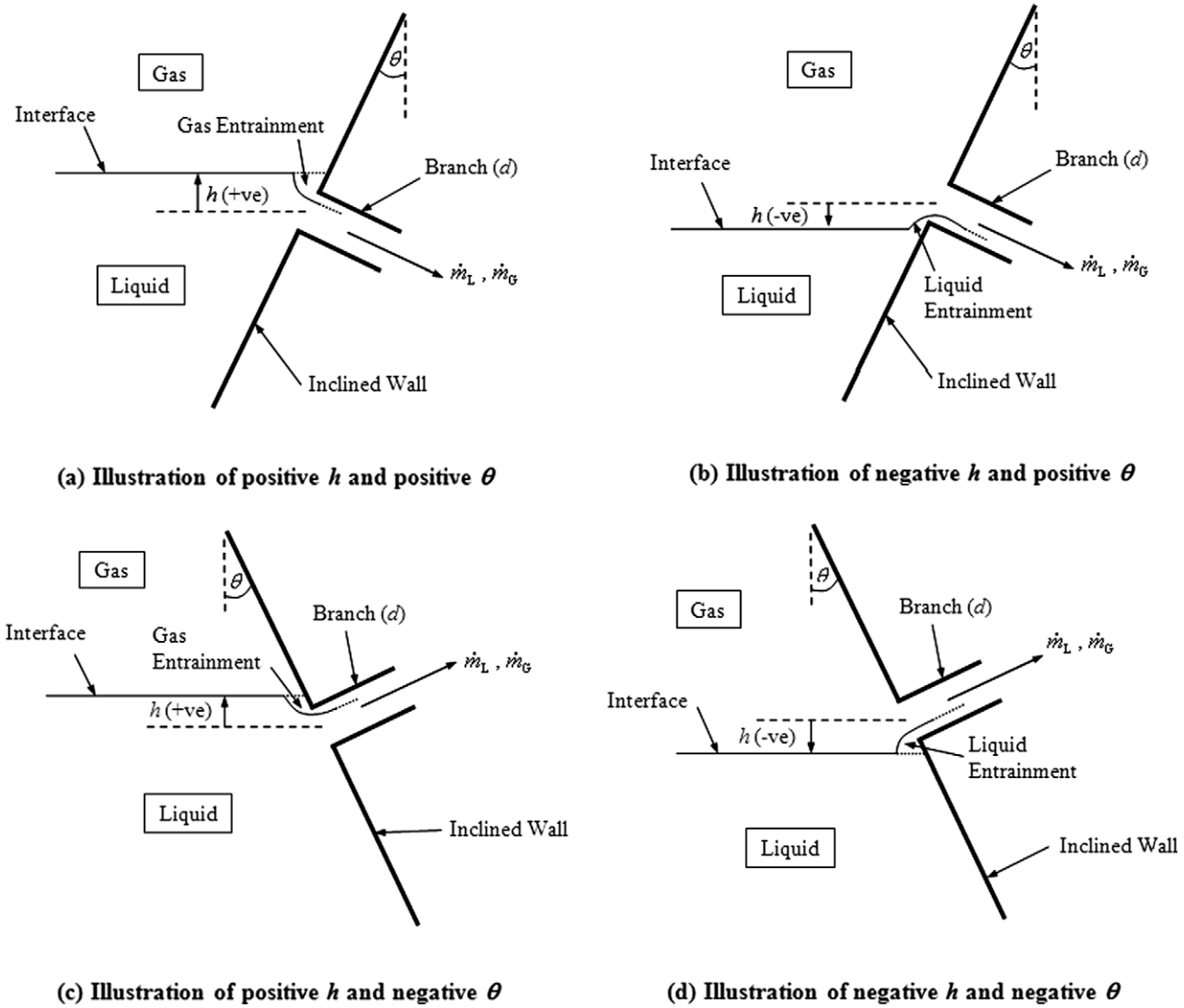

(a) Illustration of positive h and positive θ

(b) Illustration of negative h and positive θ

(c) Illustration of positive h and negative θ

(d) Illustration of negative h and negative θ

Fig. 1. Illustration of the independent parameters for positive and negative θ.

measurable amounts of liquid, $\dot{m}_L$, and gas, $\dot{m}_G$, and an expected decrease in the total mass flow rate through the branch, $\dot{m}_{TP}$, where $\dot{m}_{TP} = \dot{m}_L + \dot{m}_G$. This trend continues until the flow rate of liquid approaches zero and the flow rate of gas reaches a maximum value. This condition is referred to as the onset of liquid entrainment (OLE) at which, $h = h_{OLE}$ and $\dot{m}_G = \dot{m}_{G,OLE}$. Also, at this point, the value of $\dot{m}_G$ becomes essentially independent of any further lowering of the interface.

Bartley et al. (2008) investigated the two onsets (OGE and OLE) for the present system and developed relationships in the form: $h_{OGE}/d = g_1(Fr_L, \theta)$ and $|h_{OLE}|/d = g_2(Fr_G, \theta)$, where Fr_L and Fr_G are the Froude numbers for single-phase flow of liquid and gas, respectively. Therefore, obtaining experimental data and correlations for the mass flow rate, $\dot{m}_{TP}$, and quality, x $(= \dot{m}_G/\dot{m}_{TP})$ between OGE and OLE completes the information about the two-phase flow system shown in Fig. 1.

2.2. Experimental apparatus

A schematic diagram of the flow apparatus is shown in Fig. 2. The apparatus used in the present study was the same as that used in the previous study by Bartley et al. (2008). A brief overview of the main features of the apparatus is given here; further details about the flow loop can be found in Bartley et al. (2008). The test section was made of type 304 stainless steel sections to create a large reservoir capable of holding a stratified mixture of distilled water and air. Both the air and water supplies entered the test section through dispersing components to prevent jetting of the flow along the axis of the test section and thus, a stable, smooth interface was established in the reservoir which facilitated the accurate measurement of h. A clear acrylic pipe section was mounted to the stainless steel section for visual observation of the flow phenomena. The outer diameter of the acrylic pipe (305 mm) was large enough to prevent visual distortion, and the length of the clear pipe section was 270 mm. The supply of air to the test section was controlled by a feed-back pressure controller, which maintained a steady pressure P_o in the test section and this pressure was monitored during operation with a calibrated pressure gauge.

The end of the clear acrylic pipe section was fastened with a stainless steel flange into which a brass block containing the discharge branch was mounted. The block consisted of two parts: a cylindrical section of 104-mm diameter and 74-mm length, and a semi-cylindrical section of 104-mm diameter and 100-mm length (see Fig. 3 of Bartley et al., 2008). The semi-cylindrical section has a flat plane of dimensions 104 mm × 100 mm that is coincident with the axis of rotation of the cylindrical part. The entire brass-block insert was designed to be rotated about the cylinder's centreline to give any desired angle of inclination θ of the plane surface relative to the vertical direction. Angles of rotation of the brass block were accurately marked on the outer circumference of the brass cylinder (0°–360°) for setting the angle of inclination of the flat plane.

The discharge branch was a hole of diameter $d = 6.35$ mm machined at the centre of the flat plane perpendicular to this surface. The outer edge of the branch inlet was at a distance of at least $7.4d$ from the edges of the flat plane. The hole was machined to a depth of 32 mm (i.e., $5d$) at which point it joined at right angles with a slightly larger-diameter hole that was machined through the entire length of the cylindrical section and half-way through the semi-cylindrical section of the brass block. The arrangement consisting of the machined branch, of diameter d, and the larger-diameter hole machined parallel to the centreline of the brass block allowed flow from the test section to other components downstream for separating the flow and measuring the rates of flow of both gas and liquid.

Two thermocouples were installed to measure the temperatures of air and water in the test section at stagnation conditions. The thermocouples were mounted on the discharge flange, next to the acrylic pipe section. It should be noted that all experiments in this investigation were done at, or near, room-temperature conditions. Two pressure taps were also installed on the outlet flange, one on the air side and one on the water side, and connected to a calibrated differential-pressure transducer to facilitate measuring the position of the air–water interface, from which the value of h was determined.

Flow from the test section through the branch was directed to a separation tank, which was maintained at pressure P_s. The water was withdrawn from the bottom of the separation tank and passed to a bank of calibrated water rotameters, which was capable of measuring flow rates from 0.011 to 40.61 L/min. After

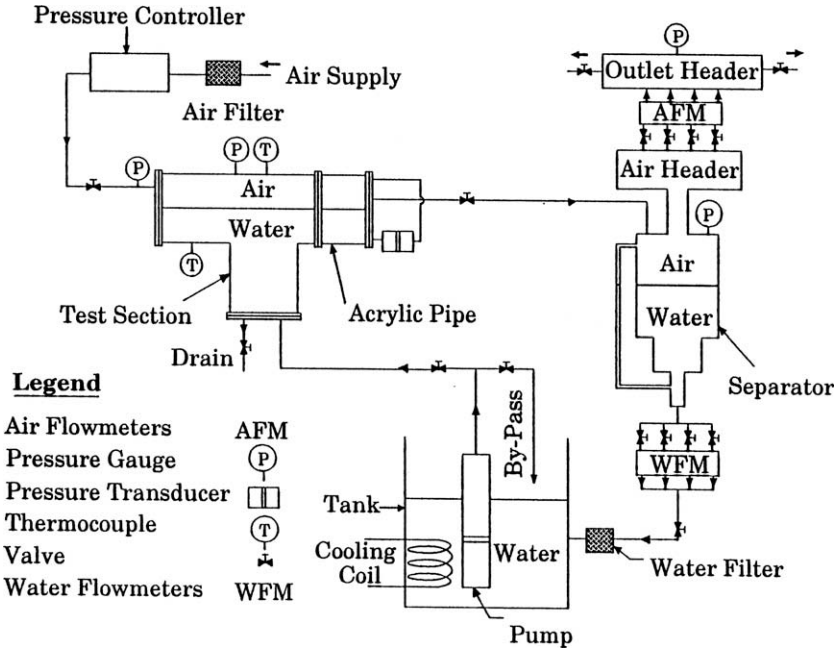

Fig. 2. Schematic diagram of the experimental test facility.

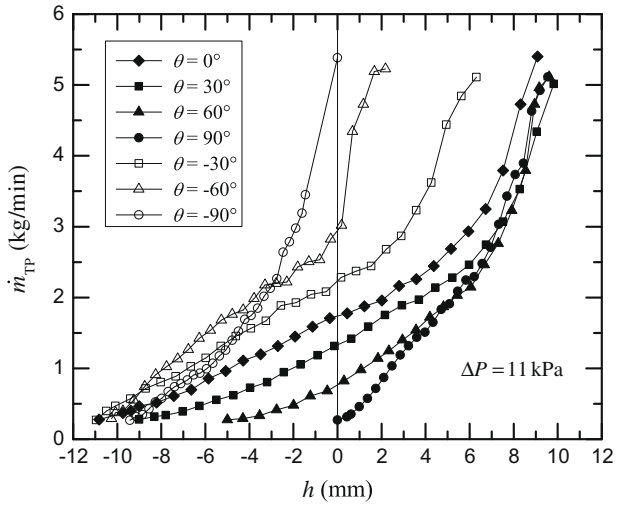

Fig. 3. Experimental data for $\dot{m}_{TP}$ at low ΔP.

measurement, the water was then returned through a filter to the main supply reservoir. The air was taken from the top of the separation tank to a header and then to a bank of calibrated air rotameters, which was capable of measuring flow rates from 0.74 to 1346 Standard L/min. The temperature of the air flow through the rotameters was measured using a thermocouple installed just upstream of the rotameter bank and the pressure of the air flow was measured at the air outlet header using a water-filled manometer.

2.3. Test conditions and experimental procedure

The experiments were conducted at room temperature ($T_o \approx 20$ °C) and a steady stagnation pressure $P_o = 316$ kPa. The test matrix included two pressure differentials, $\Delta P = 115.5$ kPa and $\Delta P = 11.0$ kPa, and seven inclination angles, $-90^o \leqslant \theta \leqslant 90^\circ$, with an interval of 30°. For each combination of ΔP and θ, the flow rates of water and air were measured over a range of discrete air–water interface heights, h, between h_{OGE} and h_{OLE}. Between 20 and 24 data points were obtained, in addition to the OGE and OLE points, at various interface heights for each of the 14 combinations of ΔP and θ. The interface level, h, was held constant for each one of these data points. Values of h_{OGE} and h_{OLE} were obtained using the procedure outlined in Bartley et al. (2008), and values of $\dot{m}_{L,OGE}$ and $\dot{m}_{G,OLE}$ were also measured to complete each data set.

At $\theta = -90°$, the procedure was largely the same as described above; however, as the gas–liquid interface became close to the plane surface of the brass block, it was observed that the liquid suddenly filled the gap between the interface and the plane surface at which point the discharge flow became single-phase liquid (even though $h \neq 0$). It is believed that this sudden jump of the interface was due to surface-tension effects. The measured liquid flow rate at this condition was taken as $\dot{m}_{L,OGE}$ and the theoretical limit $h_{OGE} = 0$ was assumed. Similarly, at $\theta = 90°$, as h became very small the flow rate of liquid entering the branch also became small until further lowering of the level of the air–water interface resulted in single-phase gas flow in the branch, even though h was slightly greater than zero. The measured gas flow rate at this condition was taken as $\dot{m}_{G,OLE}$ and the theoretical limit $h_{OLE} = 0$ was assumed.

There was a minor change to the procedure for measuring the two-phase discharge for $\theta = 60°$ and $\Delta P = 115.5$ kPa. At this particular combination of θ and ΔP, a vortex-like mode of gas entrainment occurred at relatively large values of h ($\approx 6d$ above the branch centre). During this mode of gas entrainment, a stable gas cone was visible; however, the measured gas flow rate was small. This vortex-like mode of gas entrainment persisted as the air–water interface was lowered down to $h \approx 2.5d$, at which point a transition to vortex-free gas entrainment occurred and the amount of gas entrained began to increase markedly as the interface was lowered further. Values of $\dot{m}_G$ and $\dot{m}_L$ were obtained at various values of h within both the vortex-like and the vortex-free modes.

2.4. Estimates of experimental uncertainty

Estimates of the uncertainties in the independent and dependent variables were made in the manner described in Moffat (1988) and Kline and McClintock (1953). All uncertainties quoted here are at "odds" (as used by these authors) of 20–1. The uncertainties are meant to accommodate: the accuracy of the calibrating device, the error in fitting an equation (for computer data reduction) to the calibration data, discrimination uncertainties in the measuring instruments, and unsteadiness in the process. The pressure gauges were calibrated using a deadweight tester, thermocouples (at the ice point, boiling point, and room temperature) using thermometers with discrimination of 0.05 °C, gas rotameters using wet-test flow meters and venturi meters (in turn the calibrations of which are traceable to NIST standards), and liquid rotameters using a weigh-and-time method. The pressure transducer used for measuring h was calibrated against a micro-manometer and the digital voltmeter used in the calibration was subsequently used in the normal running of the experiments. For both calibration and subsequent experiments, the sensitivity of the pressure transducer was approximately 48 mV/mm of water and the discrimination on the digital voltmeter was ±1 mV. The results of the uncertainty analysis are given in Table 1.

3. Results and discussion

3.1. Experimental data

The experimental data for $\dot{m}_{TP}$ and x at all the inclination angles ($-90^o \leqslant \theta \leqslant 90^\circ$) are shown in Figs. 3 and 4, respectively, for $\Delta P = 11.0$ kPa, and in Figs. 5 and 6, respectively, for $\Delta P = 115.5$ kPa. Considering first the $\dot{m}_{TP}$-data for the positive inclinations in Figs. 3 and 5, it can be noted that the data points agglomerate together at high values of h near the OGE suggesting that $\dot{m}_{TP}$ is not significantly influenced by θ near $h = h_{OGE}$. However, at lower interface levels, the data points for different θ spread out suggesting a strong influence of θ on $\dot{m}_{TP}$. The reason for the data agglomeration at high h is that the gas entrainment for positive angles takes place in the form of a gas cone stretching directly from the interface to the branch without touching the wall (see Fig. 9 of Bartley et al., 2008) and therefore, the inclination angle has little effect on h_{OGE} and $\dot{m}_{TP}$ near the OGE. However, at lower interface levels, the entrained gas contacts the wall as it travels towards the branch, and consequently, the magnitude of $\dot{m}_{TP}$ becomes dependent on θ for a given h. If we exclude the data of $\theta = 90°$, Figs. 3 and 5 show that $\dot{m}_{TP}$ decreases monotonically as θ increases from 0° to 60°, except for the region near the OGE. The data of $\theta = 90°$ differ from

Table 1
Measured parameters and their uncertainties.

Parameter	Uncertainty
Test-section absolute pressure, P_o	±0.9%
Separator absolute pressure, P_s	±0.7%
Gas flow rate, $\dot{m}_G$	±4.0%[a]
Liquid flow rate, $\dot{m}_L$	±2.4%[a]
Temperature, T	±0.25 °C
Interface height, h	±0.13 mm[a]

[a] Maximum uncertainty.

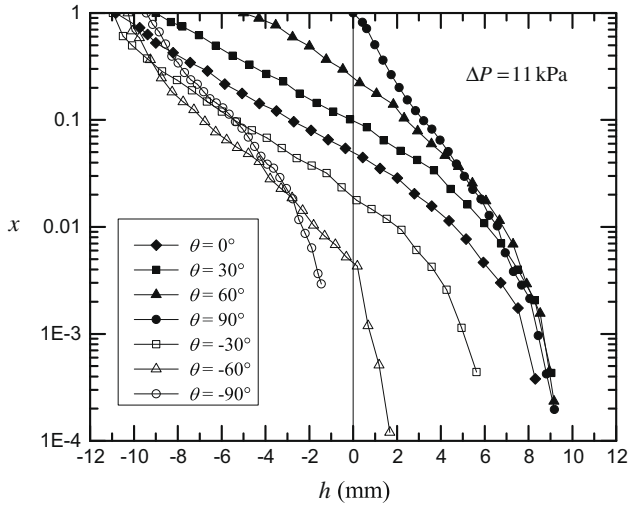

Fig. 4. Experimental data for x at low ΔP.

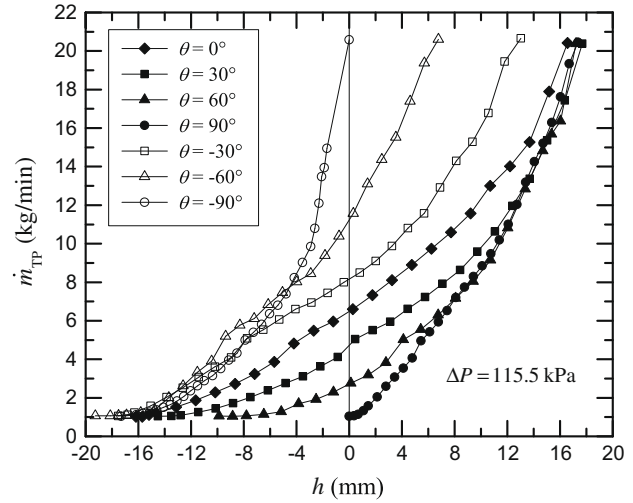

Fig. 5. Experimental data for $\dot{m}_{TP}$ at high ΔP.

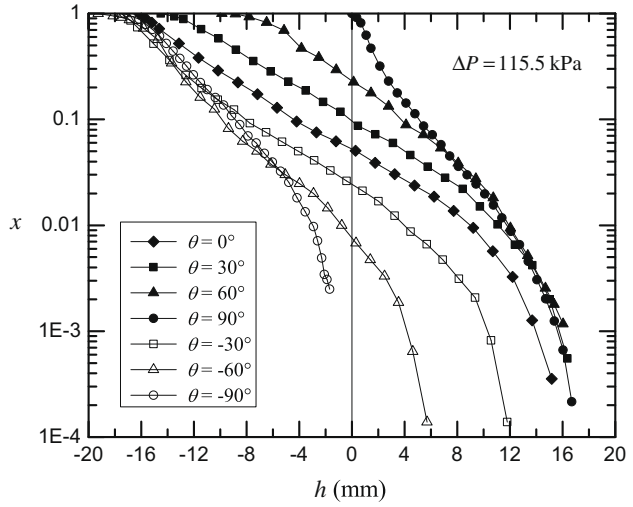

Fig. 6. Experimental data for x at high ΔP.

those of $0^o \leqslant \theta \leqslant 60^o$ in that the interface is always parallel to the outlet flat plane and the gas entrainment takes place in the form of a gas cone stretching directly from the interface to the branch at all values of h. The data line for each θ ends at the OLE point, where it has been shown earlier (Bartley et al., 2008) that θ has a strong effect on h_{OLE} for the positive inclination angles. It must be pointed out that the data corresponding to the vortex-like mode of gas entrainment at $\theta = 60°$ have been removed from Fig. 5; all the data in Figs. 3–6 correspond to vortex-free gas entrainment.

The $\dot{m}_{TP}$-data for the negative inclinations in Figs. 3 and 5 have an inverted mirror-image trend opposite to that of the data for positive angles. The data points agglomerate together near the OLE suggesting that $\dot{m}_{TP}$ is not significantly influenced by θ near $h = h_{OLE}$. That is because the liquid entrainment for these inclinations takes place in the form of a liquid spout rising directly from the interface to the branch inlet (see Fig. 5 of Bartley et al., 2008) and therefore, the inclination angle has little effect on h_{OLE} and $\dot{m}_{TP}$ near the OLE. However, at higher interface levels, the data points for different values of negative θ spread out suggesting a strong influence of θ on $\dot{m}_{TP}$. Excluding the data of $\theta = -90°$, where liquid entrainment is always via a liquid spout rising directly from the interface to the branch inlet, Figs. 3 and 5 show that $\dot{m}_{TP}$ increases at a given value of h as $|\theta|$ increases. The data line for each θ ends at the OGE-point, where it has been shown earlier (Bartley et al., 2008) that θ has a strong effect on h_{OGE} for the negative inclination angles.

The data for the discharge quality, x, shown in Figs. 4 and 6, follow a similar trend as that of the $\dot{m}_{TP}$ -data. For positive angles, the data points agglomerate near the OGE and spread out at lower interface levels, while the data for negative angles agglomerate near the OLE and spread out at higher interface levels. Excluding the data of $\theta = \pm 90°$ where the patterns of gas and liquid entrainment do not change with h, Figs. 4 and 6 show that the essential trend is that x at any given h decreases monotonically as θ changes from +60° to −60°, except for the regions near the OGE and OLE.

The characteristics observed in the $\dot{m}_{TP}$-data mentioned above are very similar between $\Delta P = 11.0$ kPa (Fig. 3) and $\Delta P = 115.5$ kPa (Fig. 5), and there exists the expected difference in the scale of the data between the two pressure-drop conditions. As well, the characteristics observed in the x-data (Figs. 4 and 6) are reasonably similar between the two pressure-drop conditions. It is reasonable to expect therefore that a normalization of the variables h and $\dot{m}_{TP}$ would be a suitable approach for correlating the data. Obtaining a correlation for predicting x and $\dot{m}_{TP}$ for any angle θ was a major objective of this study and this is presented and discussed later.

3.2. Comparisons with existing models and correlations

Several models and correlations were reported in the literature for predicting the discharge quality, x, in small branches attached to large pipes carrying a two-phase flow. These studies considered horizontal side branches ($\theta = 0°$), vertically upward branches ($\theta = -90°$), and vertically downward branches ($\theta = 90°$) and a different correlation or model was developed for each branch orientation. In most cases, the experiments on which these models and correlations were based involved flow in the main pipe parallel to the branch inlet, while in the present experiment, the two-phase mixture in the test section (upstream of the branch) was essentially stagnant.

Schrock et al. (1986) developed three empirical correlations of x for the three branch orientations and the comparison between these correlations and the present data is shown in Fig. 7. There are two sets of data for each branch orientation; one corresponding to $\Delta P = 11.0$ kPa and the other for $\Delta P = 115.5$ kPa. It is clear from the figure that the correlation for $\theta = 0°$ does reasonably well (within ±25%) at predicting the present data in the range from $0.035 < x < 1$. For $\theta = \pm 90°$, the correlations of Schrock et al. over-predict a majority of the data by a large degree over most

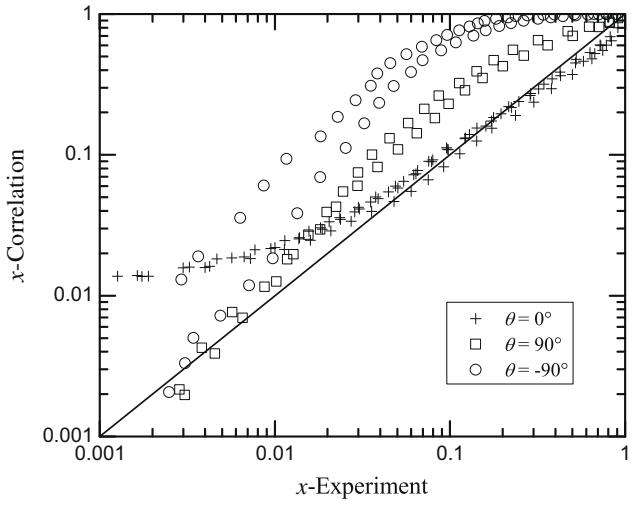

Fig. 7. Comparison between the present data and the correlation of Schrock et al. (1986).

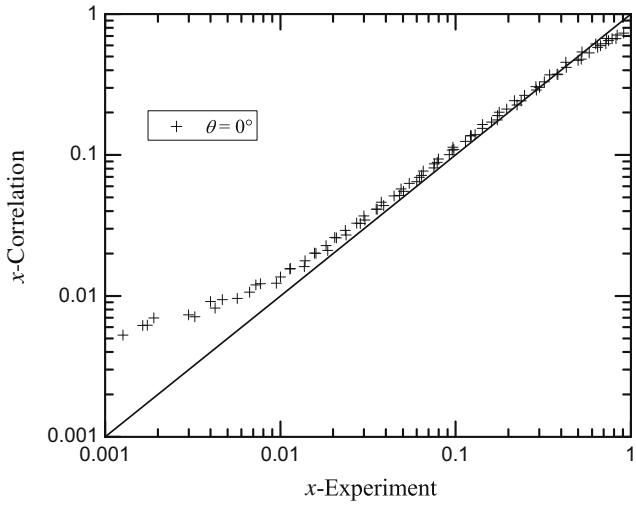

Fig. 9. Comparison between the present data and the model of Gardner (1988).

of the range of x, although their predictions for $\theta = 90°$ appear to be better than those of $\theta = -90°$. It was noted by Schrock et al. that their results for h_{OLE} (at $\theta = -90°$) did not agree with those of Smoglie and Reimann (1986) but offered no explanation for this discrepancy.

The empirical correlations of x developed by Smoglie and Reimann (1986) and Smoglie et al. (1987) are compared with the present data in Fig. 8. Their correlation for upward branches was found to over-predict the present data by very large amounts; however, since this correlation was based on limited data of high qualities ($x > 0.95$) that included slugging in the main pipe, it was decided to exclude this part of the comparison from Fig. 8. A fair agreement can be seen in Fig. 8 for $\theta = 0°$ with the correlation over-predicting the data by approximately 30% between $x = 0.04$ and $x = 1$, and by more than 30% for $x < 0.04$. The correlation for $\theta = 90°$ (using our measured values of h_{OGE}) is in good agreement with the present data, even at very small x-values. In the paper by Smoglie and Reimann (1986), it can be noted that the x-correlation for $\theta = 0°$ was based on data that had a minimum value of $x \approx 0.01$, while for $\theta = 90°$, the data extended to below $x = 0.001$. Based on these observations and the fact that their flow arrangement was different from the present one, it is fair to conclude that the comparison shown in Fig. 8 is quite satisfactory.

For a horizontal branch mounted on the side of a vertical tank, Gardner (1988) developed a purely theoretical model that relates the interface height, h, to the flow rates of gas and liquid through the branch. The final equation of the model was rearranged and solved iteratively for the quality x at any given h. A comparison between the predictions of Gardner's model and the present experimental results for $\theta = 0°$ is shown in Fig. 9. The model is in good agreement with the data (within ±20%) over the range $0.05 \leqslant x \leqslant 0.91$; but the deviation increases outside this quality range, particularly in the low quality region. Gardner's model assumes established gas and liquid flows in the branch pipe and this is probably why the model does not work as well near the two onset points.

Empirical correlations for x, developed by Micaelli and Memponteil (1989) and Maciaszek and Micaelli (1990), were also compared with the present experimental data for the three inclination angles, as shown in Fig. 10. At $\theta = 0°$, the agreement is good, particularly for $x < 0.08$, while for $x > 0.08$, the over-prediction is within 25%. On the other hand, there is significant disagreement between the predicted x and the measured values for $\theta = 90°$ in the region $x < 0.1$, and for $\theta = -90°$ over most of the range of x.

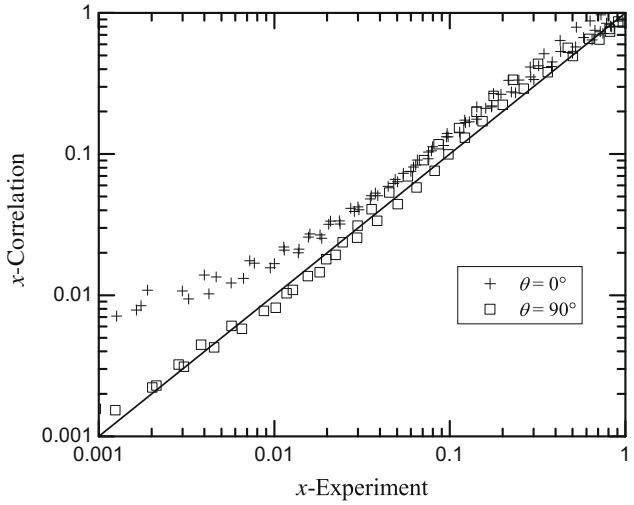

Fig. 8. Comparison between the present data and the correlation of Smoglie and Reimann (1986) and Smoglie et al. (1987).

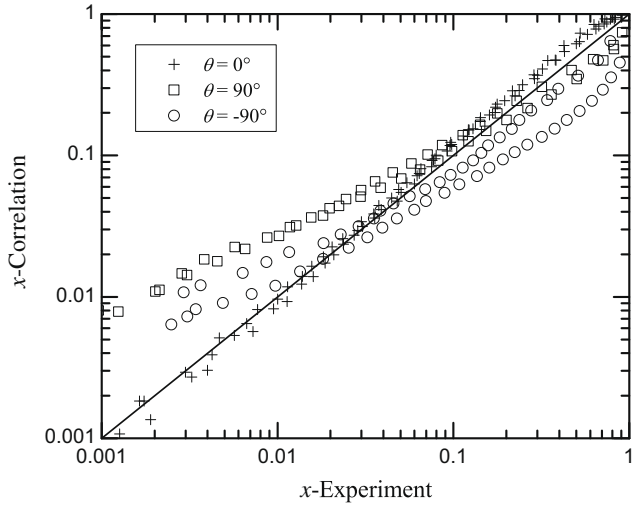

Fig. 10. Comparison between the present data and the correlation of Micaelli and Memponteil (1989).

The comparison with the theoretical models of Yonomoto and Tasaka (1991) for all three branch orientations is shown in Fig. 11. For $\theta = \pm 90°$, the data are predicted to within 30% over the range $0.02 \leqslant x < 1$. Larger deviations can be seen in Fig. 11 for $x < 0.02$. For the horizontal branch, the data are predicted to within 30% over the range $0.01 \leqslant x \leqslant 0.18$ and larger than 30% deviations were obtained outside this quality range. These observations are consistent with those of Yonomoto and Tasaka in that they noted disagreement between their model and experimental data for $\theta = 90°$ for $x < 0.02$ and they noted that their model is not appropriate near the onset points.

Welter et al. (2004) developed a theoretical model for the discharge quality in a vertically upward branch based on a potential flow simplification. The comparison between the predictions of this model and the present data for $\theta = -90°$ is shown in Fig. 12. Generally, the agreement is good, particularly in the range of quality $0.2 < x < 1$, where the experimental data are under-predicted by 30% or less. Large deviations (over 30%) can occur at low qualities ($x < 0.02$).

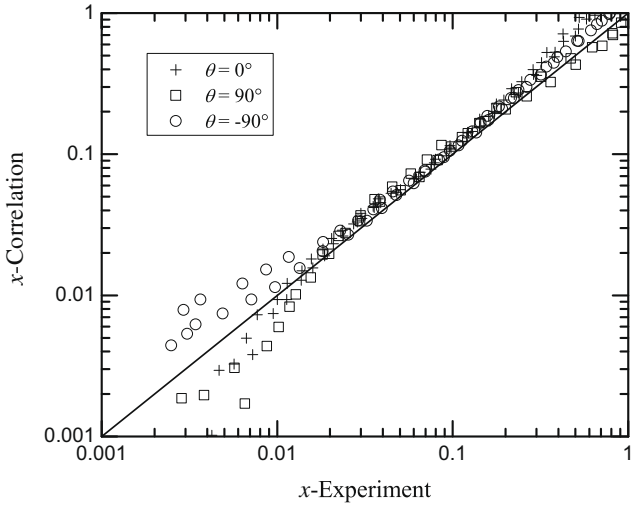

Fig. 11. Comparison between the present data and the model of Yonomoto and Tasaka (1991).

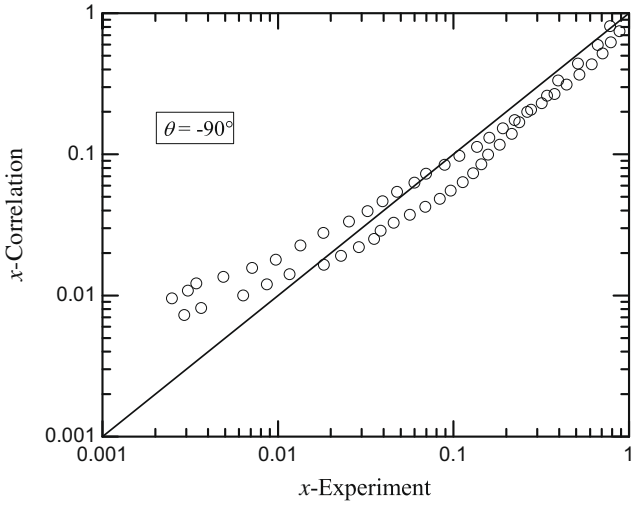

Fig. 12. Comparison between the present data and the model of Welter et al. (2004).

3.3. Data correlation

For the fixed fluid properties of air and water at the test-section pressure (P_o) and room temperature (T_o) used in this study, the experimental data presented in Figs. 3–6 for $\dot{m}_{TP}$ and x are dependent on the hydraulic resistance of the branch (R), the interface height (h), the inclination angle (θ), and the pressure difference across the branch (ΔP). Values of R and ΔP determine the single-phase flow rates ($\dot{m}_{L,OGE}$ and $\dot{m}_{G,OLE}$) and in turn, they influence the values of $\dot{m}_{TP}$ and x.

The following dimensionless groups were introduced earlier by Hassan et al. (1996a,b, 1998):

$$H = \frac{h - h_{OLE}}{h_{OGE} - h_{OLE}}, \tag{1}$$

and

$$M = \frac{\dot{m}_{TP} - \dot{m}_{G,OLE}}{\dot{m}_{L,OGE} - \dot{m}_{G,OLE}}. \tag{2}$$

Hassan et al. demonstrated that the dimensionless groups given by Eqs. (1) and (2) were successful in absorbing the effects of R and ΔP, thus facilitating the development of empirical correlations for the data. Figs. 13 and 14 show the normalized data of M vs. H and x vs. H, respectively for $\theta = 0°$ over a wide range of ΔP. These figures show that any effect on the normalized data due to changes in ΔP was barely discernible, thus confirming that the influence of ΔP has been largely absorbed by the normalization. The parameter R was not varied in the present study; however, it will be assumed, based on the results of Hassan et al., that the normalized parameters absorb the effect of R as well.

The normalization procedure mentioned above was applied to all the data and a sample of these results is shown in Figs. 15 and 16 for $\theta = \pm 30°$ and $\Delta P = 11.0$ and 115.5 kPa with an additional data set for $\theta = +30°$ using an intermediate pressure drop of $\Delta P = 42.5$ kPa. In general, the effect of ΔP on the normalized data appears to be small, particularly in the plot of x vs. H (Fig. 16). A similar result (of small ΔP effect on the normalized data) was obtained for all positive inclination angles. The effect of ΔP on the normalized data for $\theta = -60°$ and $\theta = -90°$ was somewhat larger; however, this effect did not impact significantly on the overall accuracy of the correlation, as shown later.

It can be noted from Figs. 15 and 16 that the effect of θ on the normalized parameters remains with a clear separation between the data sets of $\theta = +30°$ and $\theta = -30°$. Lines of best fit were

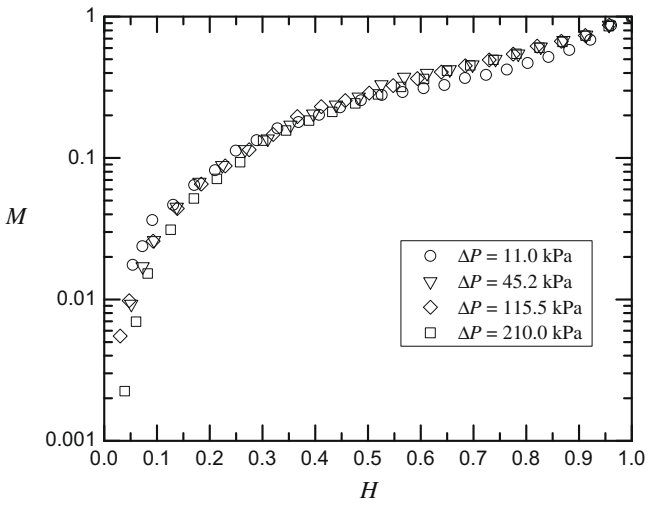

Fig. 13. Normalized M–H data for $\theta = 0°$.

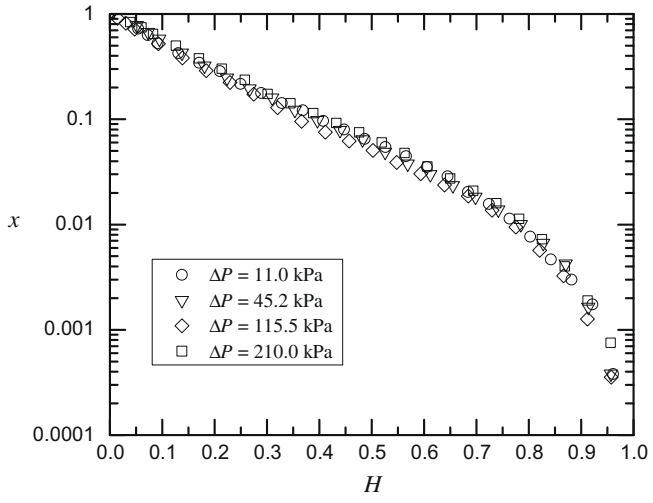

Fig. 14. Normalized x–H data for $\theta = 0°$.

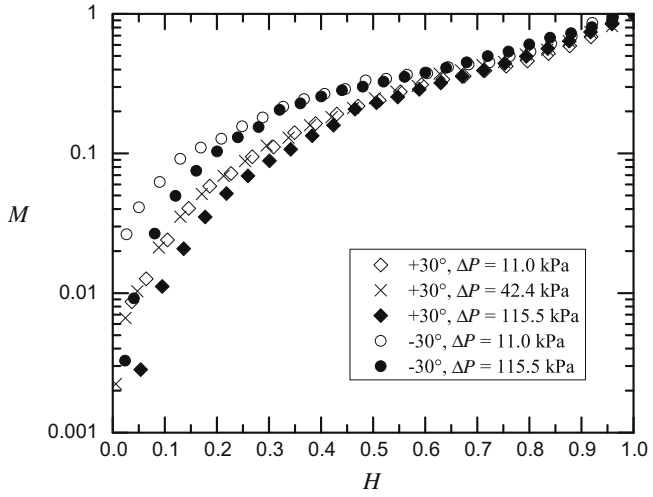

Fig. 15. Normalized M–H data for $\theta = \pm 30°$.

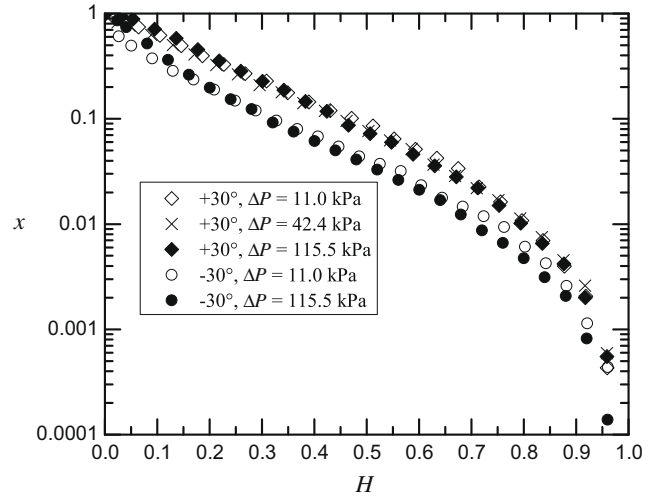

Fig. 16. Normalized x–H data for $\theta = \pm 30°$.

obtained for each inclination and the results for M and x are shown in Figs. 17 and 18, respectively. These results show a monotonic trend in the normalized data whereby the value of M was found to increase at any value of H as θ decreases from +60° to −60°, while x decreases at any value of H as θ decreases from +60° to −60°. The data of $\theta = \pm 90°$ did not follow this trend. It was noted from Figs. 3–6 that the data of $\theta = \pm 90°$ differ from those of $-60^o \leqslant \theta \leqslant 60^o$ in that the interface was always parallel to the outlet flat plane and the gas and liquid entrainment took place in the form of a gas cone stretching directly from the interface to the branch ($\theta = +90°$) or a liquid spout rising directly from the interface to the branch ($\theta = -90°$), respectively, at all values of h. This difference in flow mechanism caused the data of $\theta = \pm 90°$ not to follow the monotonic pattern of change obtained over the range $-60^o \leqslant \theta \leqslant 60^o$.

Based on the above results, correlating functions of the form $M = f_1(H, \theta)$ and $x = f_2(H, \theta)$ were sought to accommodate the main trends observed in the dimensionless data and to produce the correct limiting values for $x = 1$ and 0 and $M = 0$ and 1 at the limiting values $H = 0$ and $H = 1$, respectively. The relationships obtained are the following:

$$M = H^{a_M} \exp\left[-2.4H^{2.4}\left(1 - H^{0.85}\right)\right], \tag{3}$$

and

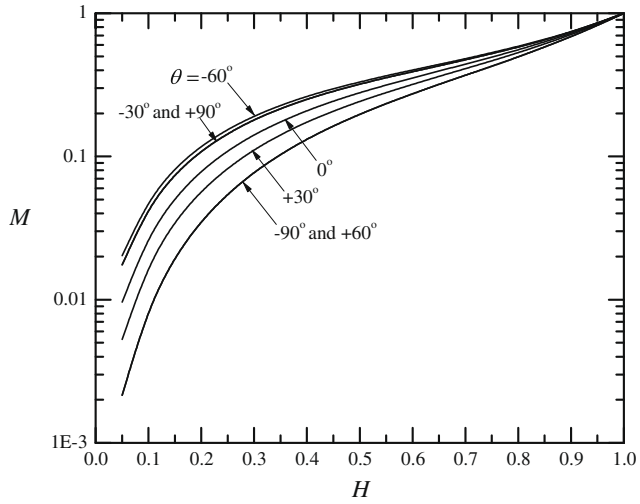

Fig. 17. Lines of best fit for M at various θ.

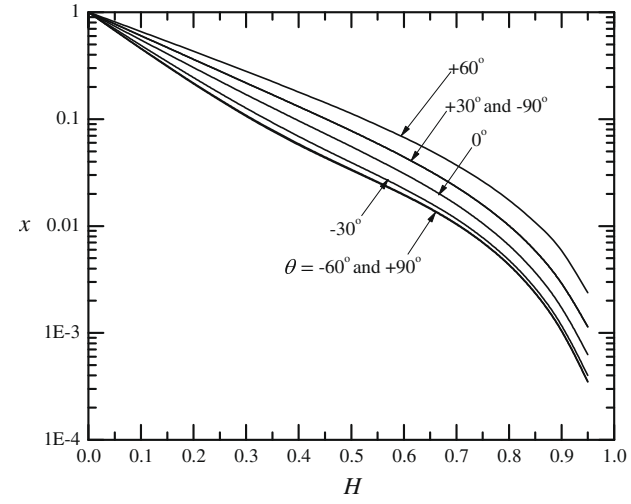

Fig. 18. Lines of best fit for x at various θ.

$$x = (1 - H)\left[0.955\exp(-a_x H) + 0.045\exp\left(-2.6H^5\right)\right] \quad (4)$$

where a_M and a_x are coefficients whose values are functions only of the inclination angle θ. The magnitudes of a_M and a_x that gave the best fit with the experimental data are shown in Fig. 19. It should be noted that a_M increases continuously and a_x decreases continuously as θ changes from $-60°$ to $+60°$, while the values of both coefficients do not follow the same trend at $\theta = \pm 90°$ for the reasons discussed in the previous paragraph.

Comparisons between the experimental data (for $\dot{m}_{TP}$ and x) and the predictions from Eqs. (3) and (4) are shown in Figs. 20 and 21. Two data sets are shown for each inclination angle; one for $\Delta P = 115.5$ kPa and the second for $\Delta P = 11.0$ kPa. Four additional data sets are shown in Figs. 20 and 21; these are for $\theta = 0°$ with $\Delta P = 45.2$ and 201.0 kPa, $\theta = +30°$ with $\Delta P = 42.4$ kPa, and $\theta = +60°$ with $\Delta P = 28.1$ kPa. Also shown in the figures are the ±30% deviation bands. In view of the complicated flow phenomena involved, the large number of relevant independent variables, the wide range of operating conditions covered in this study, and the simple form of Eqs. (3) and (4), it is fair to conclude that the agreement seen in Figs. 20 and 21 are very satisfactory. Quantitatively, the root-mean-square of the deviation between data and correlation of $\dot{m}_{TP}$ is 13.7% and the root-mean-square of the deviation between data and correlation of x is 25.6% over the range $x \geqslant 0.001$.

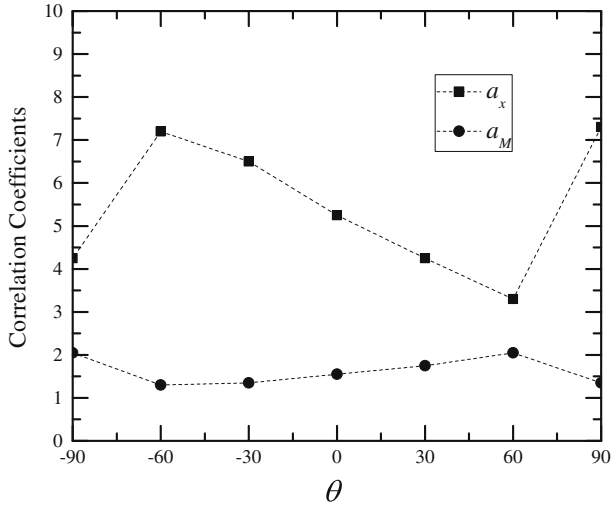

Fig. 19. Correlation coefficients.

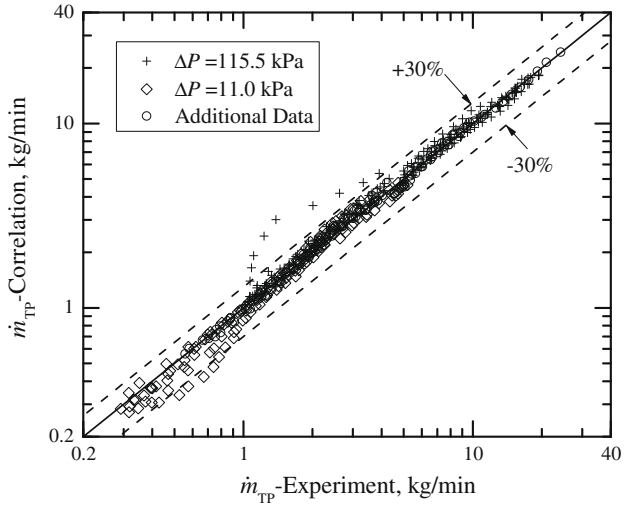

Fig. 20. Comparison between data and correlation for $\dot{m}_{TP}$.

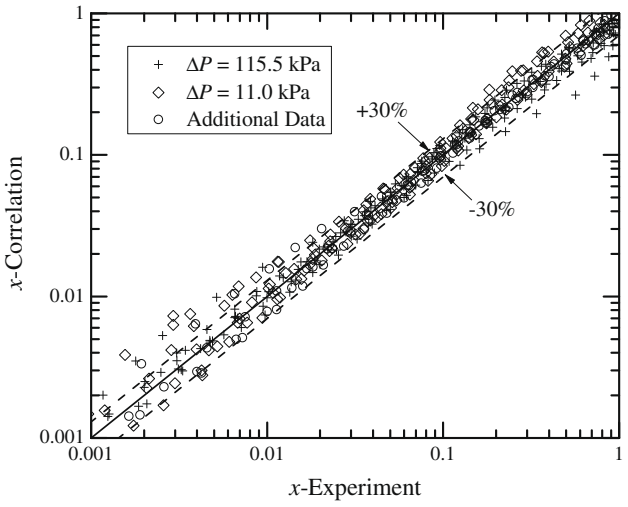

Fig. 21. Comparison between data and correlation for x.

4. Concluding remarks

New experimental data are reported for the mass flow rate and quality during two-phase discharge from a large reservoir through a small branch ($d = 6.35$ mm) under stratified conditions. The branch was machined normal to a flat plane wall that had an inclination angle θ from the vertical. The data correspond to air–water mixtures at room temperature, test-section pressure (P_o) of 316 kPa, pressure drop across the branch (ΔP) of 11.0 kPa and 115.5 kPa, and inclination angles (θ) of 0°, ±30°, ±60°, and ±90°. For each combination of ΔP and θ, the gas and liquid mass flow rates were measured at various interface heights (h) between the OGE and the OLE.

The influence of θ on the two-phase mass flow rate ($\dot{m}_{TP}$) and quality (x) was presented and discussed for both values of ΔP. It was found that the values of $\dot{m}_{TP}$ and x were not significantly influenced by θ near $h = h_{OGE}$ for positive angles and near $h = h_{OLE}$ for negative angles, and this trend was attributed to the mechanism of entrainment in these two regions. Outside these two regions, a monotonic trend was obtained, whereby $\dot{m}_{TP}$ increased and x decreased as θ decreased from +60° to −60°. The data of $\theta = \pm 90°$ did not follow this monotonic trend, again, because of the different entrainment mechanism for these angles.

Comparisons were made between the present data of the quality (x) for $\theta = 0°$ and ±90° and the predictions from existing correlations/models. It was found that the data of $\theta = 0°$ agreed well with the correlation of Micaelli and Memponteil (1989) over the whole range of x, and with the correlations of Schrock et al. (1986) over the range $0.035 < x < 1$, Smoglie and Reimann (1986) over the range $0.04 < x < 1$, Gardner (1988) over the range $0.05 \leqslant x \leqslant 0.91$, and Yonomoto and Tasaka (1991) over the range $0.01 \leqslant x \leqslant 0.18$. The data of $\theta = +90°$ agreed well with the correlation of Smoglie and Reimann (1986) over the whole range of x and with the model of Yonomoto and Tasaka (1991) over the range $0.02 \leqslant x < 1$. The data of $\theta = -90°$ agreed well with the models of Yonomoto and Tasaka (1991) and Welter et al. (2004) over the range $0.02 \leqslant x < 1$.

Normalized parameters for the mass flow rate (M) and the interface height (H), introduced earlier by Hassan et al. (1996a,b, 1998), were used in presenting the data. It was found that these parameters succeeded in absorbing the effect of ΔP on the data

and therefore, new correlations were derived expressing both M and x as functions of only H and θ. These correlations agreed well with the present data base with root-mean-square errors of 13.7% for $\dot{m}_{TP}$ and 25.6% for x over the range $x \geqslant 0.001$.

Acknowledgement

The financial assistance provided by the Natural Sciences and Engineering Research Council of Canada is gratefully acknowledged.

References

Armstrong, K.F., Parrott, S.D., Sims, G.E., Soliman, H.M., Krishnan, V.S., 1992. Theoretical and experimental study of the onset of liquid entrainment during dual discharge from large reservoirs. Int. J. Multiphase Flow 18, 217–227.

Bartley, J.T., Soliman, H.M., Sims, G.E., 2008. Experimental investigation of the onsets of gas and liquid entrainment from a small branch mounted on an inclined wall. Int. J. Multiphase Flow 34, 905–915.

Gardner, G.C., 1988. Co-current flow of air and water from a reservoir into a short horizontal pipe. Int. J. Multiphase Flow 14, 375–388.

Hassan, I.G., Soliman, H.M., Sims, G.E., Kowalski, J.E., 1996a. Discharge from a smooth stratified two-phase region through two horizontal side branches located in the same vertical plane. Int. J. Multiphase Flow 22, 1123–1142.

Hassan, I.G., Soliman, H.M., Sims, G.E., Kowalski, J.E., 1996b. Experimental investigation of the two-phase discharge from a stratified region through two side branches oriented horizontally. Exp. Therm. Fluid Sci. 13, 117–128.

Hassan, I.G., Soliman, H.M., Sims, G.E., Kowalski, J.E., 1997. Single and multiple discharge from a stratified two-phase region through small branches. Nucl. Eng. Des. 176, 233–245.

Hassan, I.G., Soliman, H.M., Sims, G.E., Kowalski, J.E., 1998. Two-phase flow from a stratified region through a small side branch. J. Fluids Eng. 120, 605–612.

Kline, S.J., McClintock, F.A., 1953. Describing the uncertainties in single-sample experiments. Mech. Eng. J. 75, 3–8.

Lee, J.Y., Hwang, S.H., Kim, M., Park, G.C., 2007. Onset condition of gas and liquid entrainment at an inclined branch pipe on a horizontal header. Nucl. Eng. Des. 237, 1046–1054.

Maciaszek, T., Micaelli, J.C., 1990. CATHARE phase separation modeling for small breaks in horizontal pipes with stratified flow. Nucl. Eng. Des. 124, 247–256.

Micaelli, J.C., Memponteil, A., 1989. Two-phase flow behaviour in a tee-junction: the CATHARE model. In: Proceedings of the 4th Int. Topical Meeting on Nuclear Reactor Thermal-Hydraulics, Karlsruhe, Germany, vol. 2, pp. 1024–1030.

Moffat, R.J., 1988. Describing the uncertainties in experimental results. Exp. Therm. Fluid Sci. 1, 3–17.

Parrott, S.D., Soliman, H.M., Sims, G.E., Krishnan, V.S., 1991. Experiments on the onset of gas pull-through during dual discharge from a reservoir. Int. J. Multiphase Flow 17, 119–129.

Schrock, V.E., Revankar, S.T., Mannheimer, R., Wang, C.H., Jia, D., 1986. Steam-water critical flow through small pipes from stratified upstream regions. In: Proceedings of the 8th Int. Heat Transfer Conf., San Francisco, California, vol. 5, pp. 2307–2311.

Smoglie, C., Reimann, J., 1986. Two-phase flow through small branches in a horizontal pipe with stratified flow. Int. J. Multiphase Flow 12, 609–625.

Smoglie, C., Reimann, J., Müller, U., 1987. Two phase flow through small breaks in a horizontal pipe with stratified flow. Nucl. Eng. Des. 99, 117–130.

Teclemariam, Z., Soliman, H.M., Sims, G.E., Kowalski, J.E., 2003. Experimental investigation of the two-phase flow distribution in the outlets of a horizontal multi-branch header. Nucl. Eng. Des. 222, 29–39.

Welter, K.B., Wu, Q., You, Y., Abel, K., McCreary, D., Bajorek, S.M., Reyes Jr, J.N., 2004. Experimental investigation and theoretical modeling of liquid entrainment in a horizontal tee with a vertical-up branch. Int. J. Multiphase Flow 30, 1451–1484.

Yonomoto, T., Tasaka, K., 1988. New theoretical model for two-phase flow discharged from stratified two-phase region through small break. J. Nucl. Sci. Technol. 25, 441–455.

Yonomoto, T., Tasaka, K., 1991. Liquid and gas entrainment to a small break hole from a stratified two-phase region. Int. J. Multiphase Flow 17, 745–765.

Zuber, N., 1980. Problems in modeling of small break LOCA. Nuclear Regulatory Commission Report NUREG-0724.